Željko Domazet[1], Francisko Lukša[1], Petra Bagavac[1]

Failure analysis of the rolling mill stand coupling

[1]Faculty of Electrical Engineering, Mechanical Engineering and Naval Architecture; University of Split; Split, Croatia
[2]Steelworks Split d.d., 21212 Kaštel Sućurac, Croatia
[3]Bit-art informatika, Split, Croatia

Abstract

The failure analysis of two slipper couplings showed that both couplings fractured as a result of fatigue. In both cases, the fracture started in the corner between the paddle and the coupling body and propagated around the corner. Both fractures were caused by the deficient design of the fillet between the paddle and the coupling body with high stress concentration. In order to extend actual service life, three design modifications were considered. Numerical analysis showed that the redesign of the coupling with stiffener between the paddle and the coupling body reduced maximum local and actual service life of couplings and can be improved from finite to infinite.

Keywords*: failure analysis; slipper coupling, fatigue*

1. Introduction

The roughing mill is one of the most loaded parts of the steel plant; it consists of two reversing 3-high mill stands with ten passes, eight on the first stand and two on the second, Fig.1. The failures of the rolls with grooves on the 1st stand of the 3-high-roughing mill stand occurred four times, Ref. [1]. The failures of the slipper coupling between the gearbox and the roughing mill occurred 2 times, Fig.2. The first coupling had been in service for 3.5 years when the coupling failure occurred. A failure of the second coupling occurred when the coupling had been in service for almost 4 years.
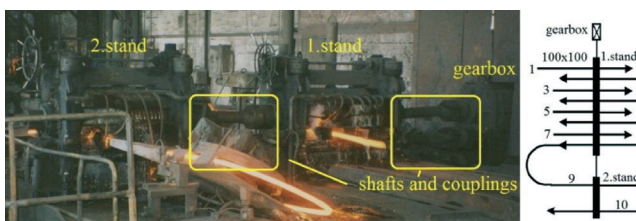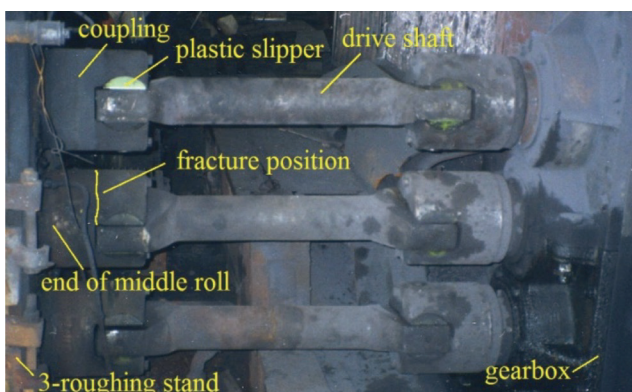
Slipper couplings and drive shafts are used to transmit torque between gearbox and 3-high-roughing mill stands. A failure of both couplings occurred on the middle roll between the first stand and the gearbox, roll side, Fig.2.

2. Failure of couplings

The couplings were made of quenched and tempered steel 30CrNIMo8 according to German standard DIN (Deutsches Institut für Normung), Ref.[2]. The chemical composition of the material was verified by using the quantometer. The hardness readings and microstructure indicated that the coupling had been satisfactorily heat treated by quenching and tempering. The fracture occurred two times in the groove between the paddle and the coupling body, Fig.3.
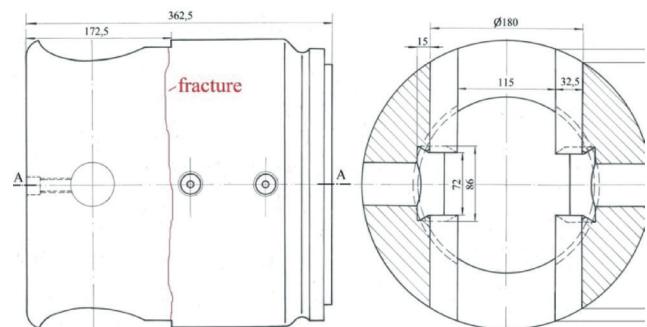

Fig. 1. Roughing mill [1]

Fig. 2. Shafts and couplings between the 3-high-roughing stand and the gearbox

Fig. 3. Coupling drawing and fracture position

2.1. Fracture surface investigation

The first broken coupling is shown in Fig.5 and Fig.6. On the fracture surface of the first coupling there are four fracture regions, Fig.6: two regions of two fracture origins (at 1 and 2), the region of progressive fatigue crack propagation with curved beach marks (at 3), and the final fast fracture zone (at 4).
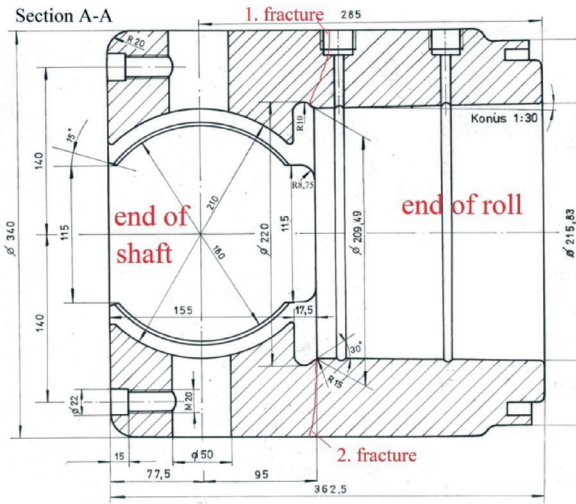
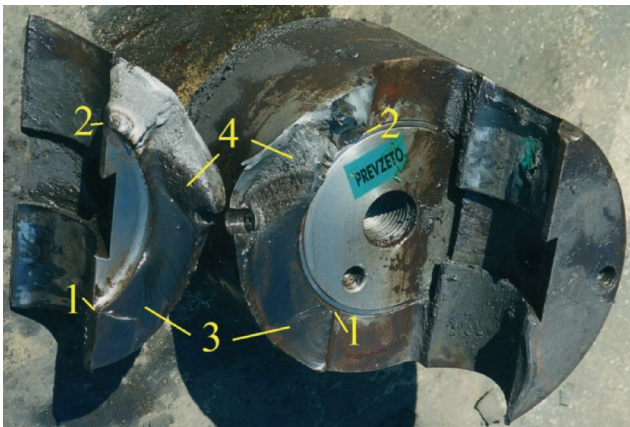**Fig. 4.** Coupling drawing – Section A and fracture position
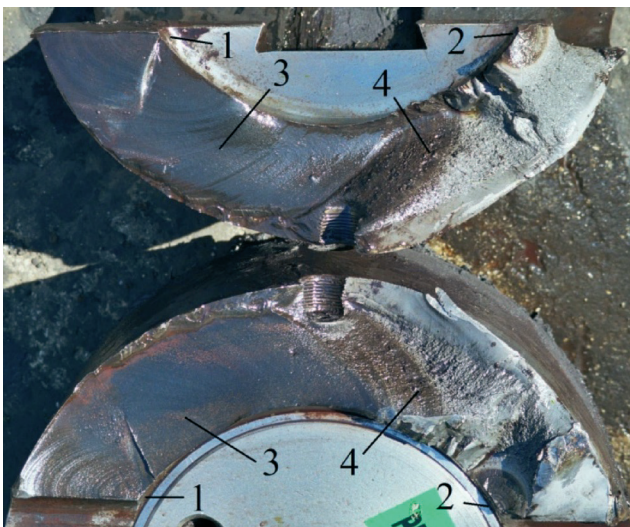

Fig. 5. Fracture of 1st coupling

Fig. 6. Fracture surface of 1st coupling

The crack started in the corner of region 1 and propagated around this corner, what can be visible with curved beach marks. The final fracture occured when the region of progressive fatigue crack propagation reached about 60% of the paddle cross section, practically connected with another weak point – oil chanel.
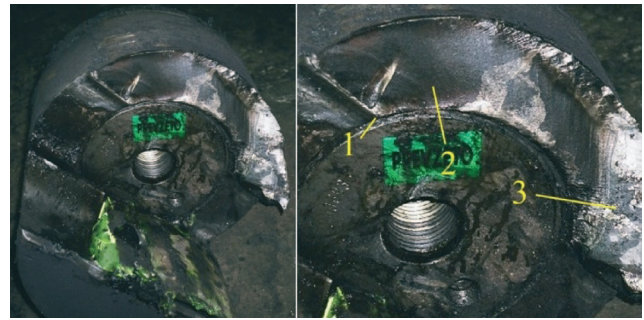
The second broken coupling is shown in Fig. 7.

Fig. 7. Fracture of 2nd coupling

A visual examination of the fracture surface of the second coupling showed three fracture regions, Fig.7: the region of fracture origin (at 1), the region of progressive fatigue crack propagation with curved beach marks (at 2), and the final fast fracture zone (at 3). In this case the crack started in the corner of region 1, similar to the previous case but on the opposite paddle. The crack propagated around the corner what is also visible with curved beach marks. The final fracture occured when the region of progressive fatigue crack propagation reached about 65% of the paddle cross seaction. The second fracture origin is not clearly expressed.

The conclusion from the surface investigation was that both couplings fractured as a result of fatigue. The fracture started in the corner between the paddle and the coupling body and propagated around the corner. In both cases the final fracture occurred when the fatigue crack propagation reached about 60-65% of the paddle cross section.

2.2. Stress analysis

2.2.1. Torque of drive shaft

The drive shafts and couplings transmit torque which consists of rolling torque required for deformation and torque required for the friction in the bearings.

The rolling stock passes between two rolls and torque required for deformation is torque of two rolls, Fig.8. The equation for rolling deformation torque, Ref. [3], is given by
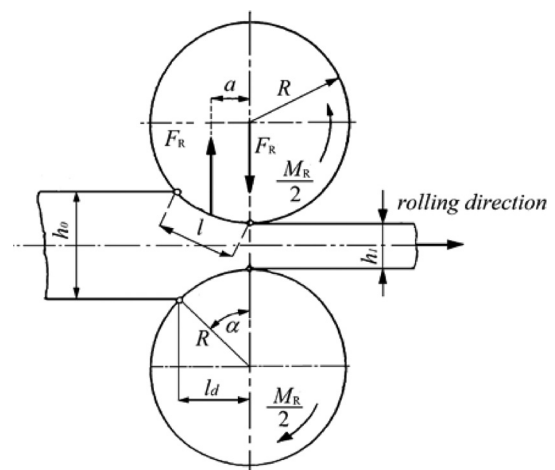

Fig. 8. Rolling force and rolling deformation torque

$$T_R = 2 \, F_R \cdot a, \qquad (1)$$

where F_R is rolling force and "a" is distance of rolling force from centre of the roll.

The distance of the rolling force from centre of the roll, Ref. [3] and [4], can be calculated as

$$a = 0.5 \cdot l_d \qquad (2)$$

where l_d is the projected length of the contact arc.

Each drive shaft transmits half of total rolling torque and torque of drive shaft can be calculated from the rolling deformation torque increased for the friction in the bearing by 10%, Ref. [3];

$$T_{sh} = 0.5 \cdot 1.1 \cdot T_R, \qquad (3)$$

where $0.5 \cdot T_R$ is half of rolling deformation torque.

2.2.2. Paddle force

The plastic slippers are installed between the coupling paddles and the driven shaft, Fig.9.

Torque is transmitted through the contact surfaces between shaft and slippers and slippers and paddles. The force acting on each paddle is resultant force of load distributed on the paddle surface from the slipper. The load distribution has trapezoidal shape, Ref. [3]. Drive shaft torque can be expressed, Ref. [3];

$$T_{sh} = F \cdot b, \qquad (4)$$

where F is resultant force of distributed load and b is distance between resultant forces, Fig.9.
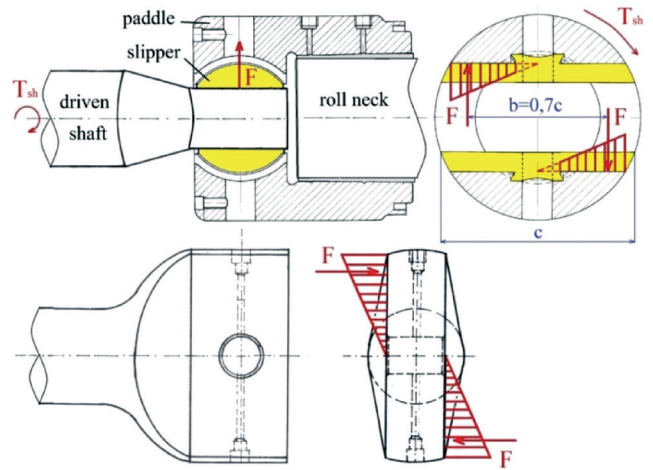

Fig. 9. Coupling load

Fig. 10. Roughing mill schema

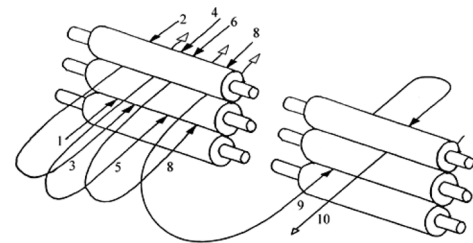### 2.2.3. Torque of middle drive shaft and paddle force change according to time

Rolling in the roughing mill consists of 10 passes in two stands, 8 in the first stand and 2 in the second stand, Fig.10. In each pass a different rolling force acts, Fig.11, and the corresponding rolling deformation torque.
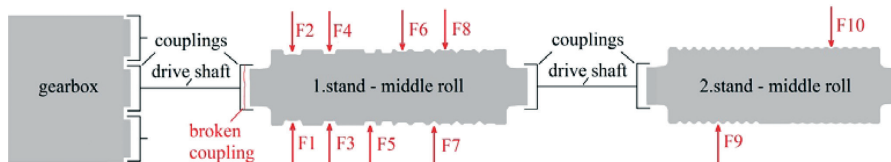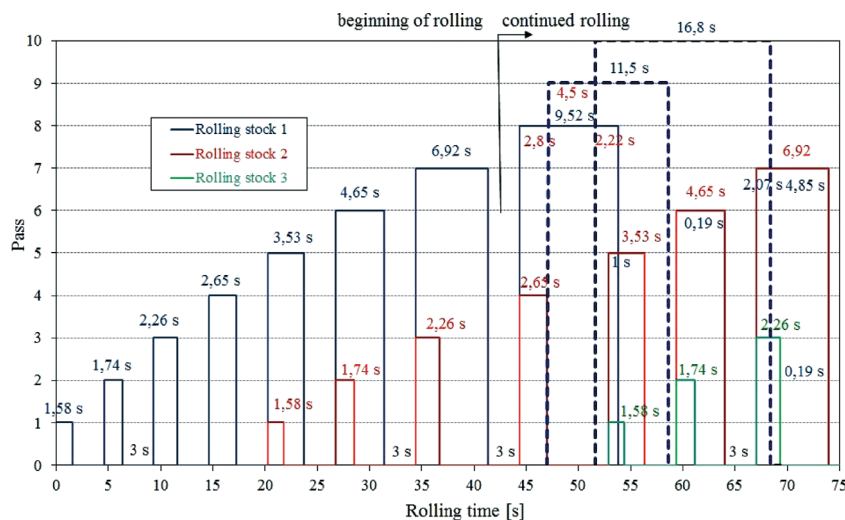

Fig. 11. Roughing mill power transmission

Fig. 12. Roughing mill rolling process

The middle drive shaft between the gearbox and the 1st stand transmits half of the total rolling torque following a rolling sequence of 8 passes in the first stand and 2 passes in the second stand, Fig.12.

The rolling process on the roughing mill begins with the rolling stock in the pass 1 and the rolling time is 1.58 seconds. Between rolling in passes, there is a rolling pause of 3 seconds because of changing the rolling direction. After the rolling pause of 3 seconds, the rolling stock comes in pass 2 and rolling time is 1.74 seconds, followed by rolling in pass 3 and pass 4. After 20 seconds of the first stock start, the rolling of two rolling stocks begins together in passes 1 and 5. The rolling of two rolling stocks together continues in passes 2 and 6, passes 3 and 7 and passes 4 and 8.

Rolling in pass 9 in the second stand starts 2.8 seconds after the first rolling stock goes out from pass 8. Then 4.5 seconds after the rolling starts in pass 9, the first stock comes in pass 10 in the second stand. The rolling of the third stock begins 53 seconds after the first stock starts and the rolling process on the roughing mill continues according to the rolling sequence and repeats until rolling stops.

The rolling process can be divided into two parts; the first part is the beginning of rolling and the second part is continued rolling, Fig.12. In regular service, the first part of the rolling process, rolling beginning, is a very short period of the total rolling in comparison with the second part, continued rolling.

Rolling deformation torque and torque of the middle drive shaft for each separate pass are obtained from Eq. (1), (2) and (3). The paddle force is obtained from Eq. (4). The results are shown in Table 1. The experimentally determined rolling forces were used for the calculation of the drive shaft torque, Ref. [1] and [5].

Table 1. Roughing mill rolling sequence, torque of the middle drive shaft and paddle force

Pass		1	2	3	4	5	6	7	8	9	10
Pass shape		box	box	box	box	box	oval	square	oval	square	oval
Groove dimensions [mm]		100x82	100x66	67x80	67x59	66x52	80x34	40	58x20	30	45x18
Cross-section [mm²]	9850	8015	6474	5398	4032	3280	2286	1578	1075	890	610
Roll working diameter [mm]		372,5	393,5	372,5	398,5	396,5	419,5	397,25	433	425	441,5
Roll speed [rpm]		120	120	120	120	120	120	120	120	120	120
Length of rolled stock [m]	3	3,69	4,56	5,47	7,33	9,01	12,93	18,73	27,49	33,20	48,44
Projected length of contact arc l_d[mm]		57,84	56,10	72,08	64,68	68,97	61,44	79,10	64,97	56,46	51,47
Rolling time [s]		1,58	1,74	2,26	2,65	3,53	4,65	6,92	9,52	11,5	16,8
Rolling pause [s]		3	3	3	3	3	3	3	3	2,8	4,5
Experimentally determined roll force [kN]		356,1	494,6	356,1	524,2	346,2	544,0	286,8	445,1	180,5	292,2
Distance of force from roll centre a[mm]		28,9	28,1	36,0	32,3	34,5	30,7	39,6	32,5	28,2	25,7
Rolling deformation torque [kNm]		10,3	13,9	12,8	17,0	11,9	16,7	11,3	14,5	5,1	7,5
Torque of middle drive shaft [kNm]		**5,7**	**7,6**	**7,1**	**9,3**	**6,6**	**9,2**	**6,2**	**8,0**	**2,8**	**4,1**
Paddle force for separate pass[kN]		**25,3**	**34,1**	**31,5**	**41,6**	**29,3**	**41,0**	**27,9**	**35,5**	**12,5**	**18,5**

The torque of the middle drive shaft change according to time, Fig.13, is constructed from the rolling process on the roughing mill, Fig.12 and the torque of the middle drive shaft for each pass, Table 1.

The diagram in Fig.13 shows that torque change follows the rolling schedule. In pass 1, the torque value was 5.7 kNm with a duration of 1.58 seconds. In pass 2 the torque value was 7.6 kNm with a duration 1.74 seconds.
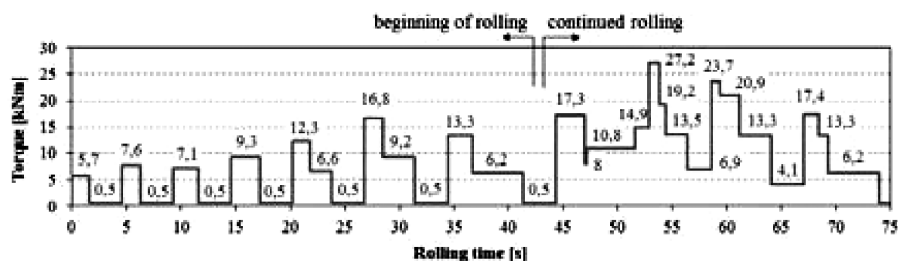

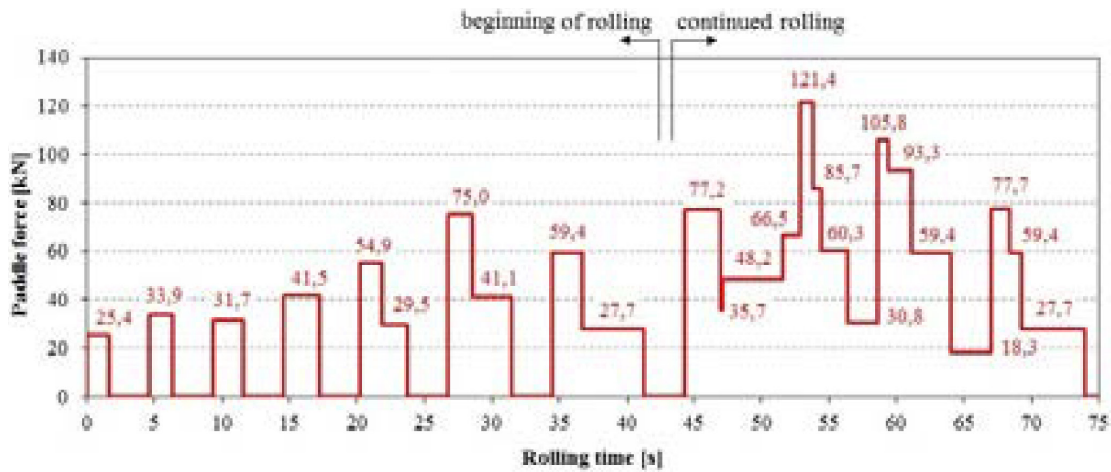**Fig. 13.** Drive shaft torque change according to time

Fig. 14. Paddle force change according to time

In pass 3 the torque value was 7.1 kNm in 2.26 seconds and 9.3 kNm in 2.65 seconds in pass 4. For rolling two stocks in pass 1 and 5 the torque value was 12.3 kNm with a duration of 1.58 seconds, which is a sum of the torque values in passes 1 and 5. Rolling in pass 1 finished after 1.58 seconds, and the torque value was 6.6 kNm with a duration of 295 seconds due to rolling in pass 5.

The paddle force change according to time, Fig.14, was made according to the roughing mill rolling schedule according to time, Fig.12, and paddle force, Table 1.

The diagram in Fig.14 shows that the maximum paddle force was 121.4kN during the rolling of three stocks together in passes 1, 5 and 8, 9 and 10 with a duration of 1 second.

2.2.4. Numerical analysis of the slipper coupling and the drive shaft

The stress analysis of the slipper coupling and the drive shaft was carried out by the finite element method using ADINA software. The linear elastic model with 3D solid elements with eight DOF per nodes was used, Fig.15 and Fig.16. Each node had 3 degrees of freedom, translation in X, Y and Z direction. The model of coupling was fixed in the contact area with the roll and loaded with trapezoidal distributed forces in the nodes on the paddle surface. The model of the drive shaft was fixed in the back side face and loaded with trapezoidal distributed forces in the nodes on the contact surfaces.

FEM analysis of the slipper coupling revealed that a force of 121.4 kN caused the maximum stress of 294
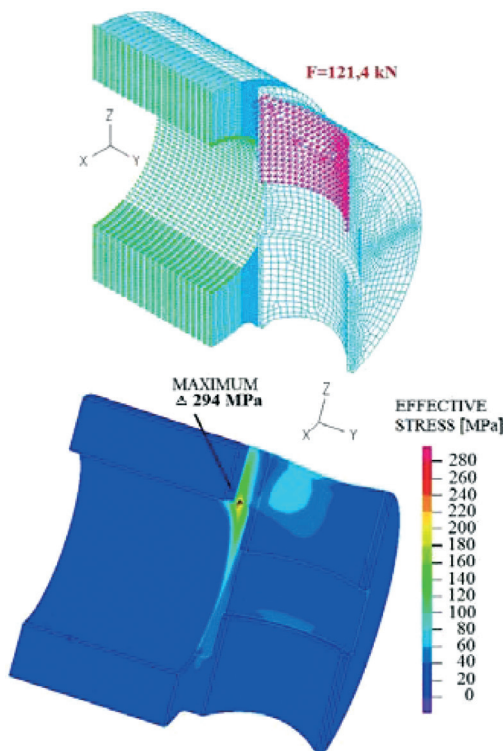

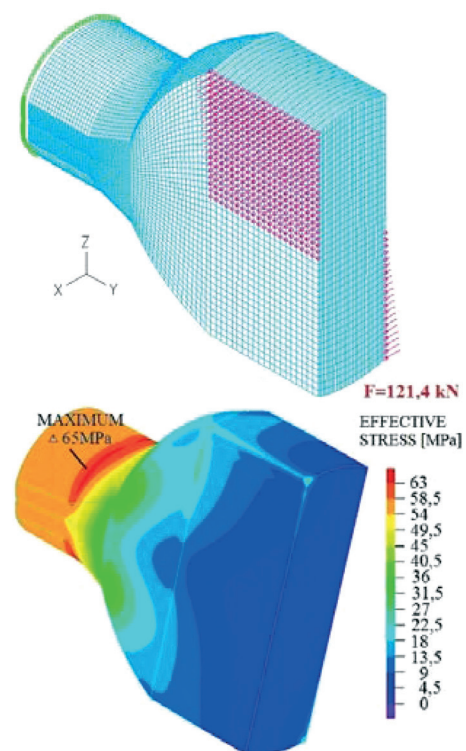**Fig. 15.** Numerical analysis of the slipper coupling

Fig. 16. Numerical analysis of the drive shaft

MPa on the fillet between the paddle and the coupling body, Fig.15, in the same place where both fractures originated. FEM analysis of the drive shaft revealed that the maximum stress of 65 MPa appeared due to change in the shaft diameter, Fig.16, and that the drive shaft was not the critical point.

3. Proposed design modifications

The analysis showed that both fractures were caused by the deficient design of the fillet between the paddle and the coupling body with high stress concentration. In order to extend the actual service life, three design modifications were considered:

a) Decreasing the stress concentration in the corner between the paddles and the coupling body by change of the fillet radius and the grove radius, Fig.17a;

b) Increasing the external diameter of the coupling in the critical place, Fig. 17b and

c) Redesign of the coupling with stiffener between the paddle and the coupling body, Fig. 17c.
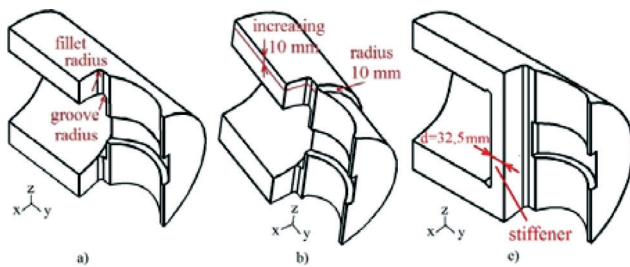

Fig. 17. Considered actions

In the first and the second solution the redesign was limited only to reshape the coupling and did not request any change of the shaft. The third solution involved also redesigning the shaft – reducing the shaft length by 100 mm.

3.1. Change of fillet and groove radius

The high stress concentration is caused by two stress raisers, the fillet and the groove in the corner between the paddle and the coupling body. The change of the fillet and groove radius was analyzed in order to reduce stress concentration. The radius of the fillet was limited by the free space necessary to move the shaft the coupling and can be increased from 8.5 mm to 10 mm, Fig.18. The radius of the groove was controlled by the groove width and the groove width could not be increased, Fig.18.

FEM analysis of local stresses revealed that a redesign by changing the radius of the fillet will slightly decrease local stresses.
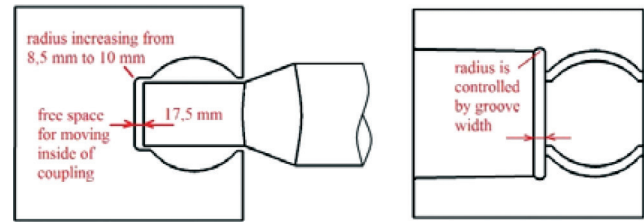

Fig. 18. The space between the shaft and the coupling

3.2. Increasing the external diameter of the coupling in the critical place

The rolls during exploitation reduce the working diameter by turning due to roll wearing. The gap between the rolls should be adjusted in the requested dimension by reducing the distance between the roll axes. Because of that, the minimum of the free space between the external diameters of two couplings was 80 mm, Fig. 19, which allowed increasing the external diameter of the coupling from 340 to 360 mm. Additional increasing the external diameter may disturb the assembly and maintenance work.
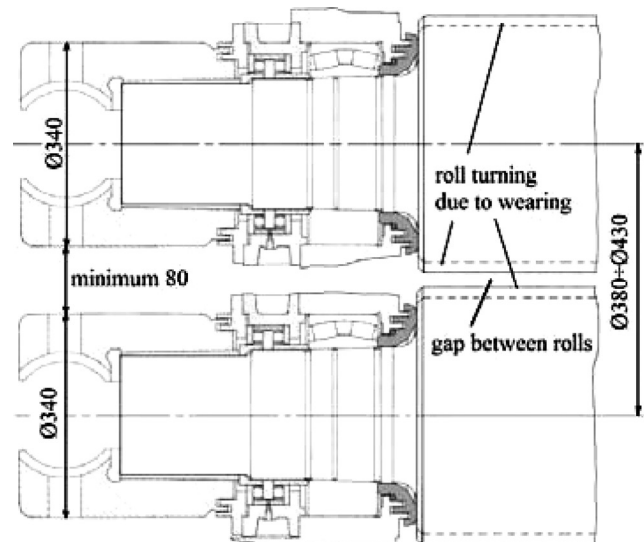

Fig. 19. Space between the external diameters of two couplings

FEM analysis of local stresses revealed that increasing the external diameter from 340 mm to 360 mm reduced the maximum local stress from 294 MPa to 251 MPa, Fig. 20.
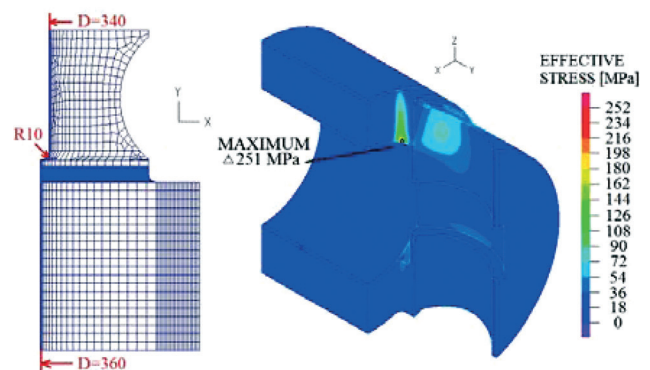

Fig. 20. FEM analysis with the increased external diameter

3.3. Redesign of the coupling with stiffener between the paddle and the coupling body

In the original design there was an interference of two stress raisers, the fillet and the groove. The redesign of the coupling with stiffener between the paddle and the coupling body was considered in order to split influences of stress raisers on local stresses. A numerical analysis of local stresses was carried out for the new design with a stiffener thickness of 12.5 mm and 32.5 mm, Fig. 21. With the new design, the distance between the fillet centre and the groove centre with a stiffener thickness of 12.5 mm was 30 mm and with 32.5 mm it was 50 mm.

FEM analysis revealed that the redesign of the coupling with a stiffener thickness of 12.5 mm reduced the maximum local stress from 294 MPa to 163 MPa (about 44%) and with a stiffener thickness of 32.5 mm it was reduced from 294 MPa to 139 MPa (about 52%).

3.4. Service life

The actual service life of couplings was estimated from the mill production and rolling schedule. The service life of the couplings was divided into the sequences depending on roll wearing. The roll service life before machining due to wearing was estimated after 4000 rolling tons of steel (about 15 working days or about 17390 rolled billets). After that period, the rolls should be replaced and machined on new working dimensions. The couplings should be dismantled and installed again after the roll machining.

Each sequence of coupling service life was also about 4000 rolling tons. During continued rolling, the drive shaft torque for one billet changed 15 times, Fig. 13. For 17390 billets the total number of the drive shaft torque changed about 260000. During one sequence of the coupling service life the maximum drive shaft torque was
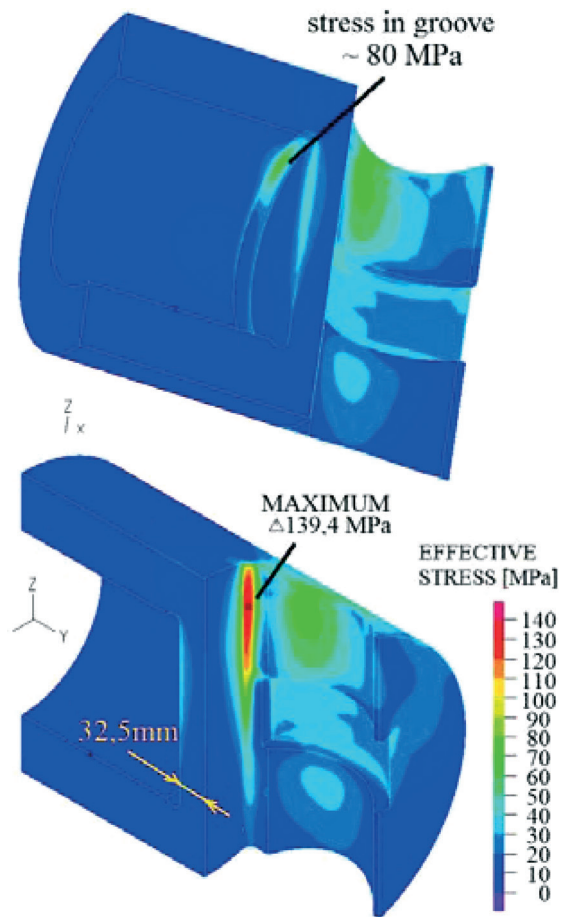

Fig. 21. FEM analysis of the new coupling design with a stiffener thickness of 32.5 mm

17390, so the number of cycles of maximum stress was also 17390.

Based on this data, the actual service life of the coupling was estimated for 27 working sequences, (469530 divided by 17390 is 27), or 405 working days (time period about 3 years), Fig. 22. The fatigue strength curve of the
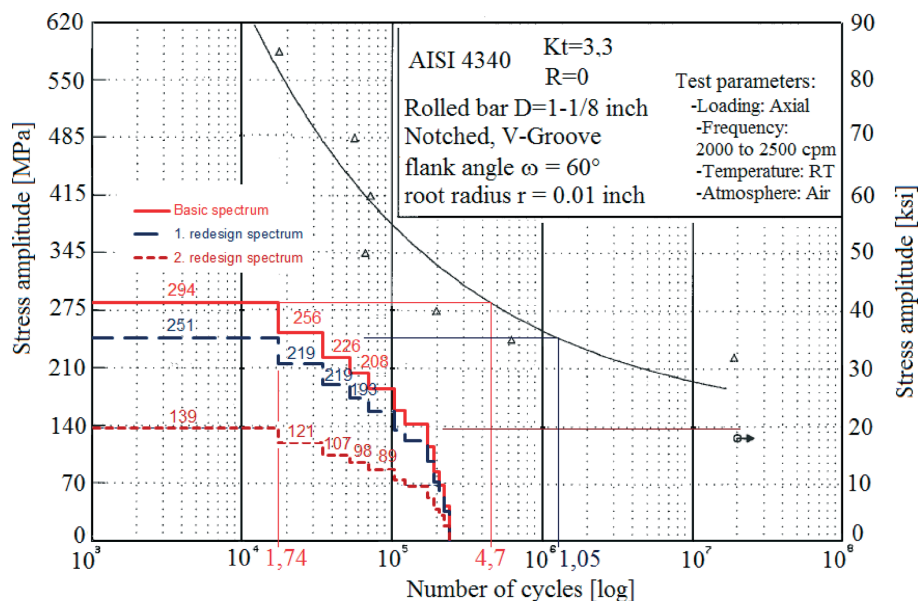

Fig. 22. Stress spectra for critical area

material was used from literature [8] for the equivalent material 4340 according to ASTM (American Society for Testing and Materials) [9].

The redesign by increasing the external diameter of the coupling in the critical place reduced the maximum local stress by about 15% (from 294 MPa to 251MPa) and increased fatigue life by about 100% according to the actual estimated fatigue life, Figure 22.

The redesign of the coupling with a stiffener between the paddle and the coupling body reduced the maximum local stress below the fatigue endurance limit (from 294 MPa to 139 MPa).

Based on this analysis, the actual service life of the shaft can be improved from the finite (about $4.7 \cdot 10^5$ cycles) to the infinite lifetime.

4. Conclusion

The failure analysis of two slipper couplings showed that both couplings fractured as a result of fatigue due to a deficient design. In both cases, a fracture started in the corner between the paddle and the coupling body, and propagated around the corner. The final fracture occurred when the fatigue crack propagation reached about 60-65% of the paddle. In the basic design, the corner between the paddle and the coupling body was the intersection of two stress raisers, the fillet and the groove.

Three design modifications were considered to avoid having high stress concentration at the corner between the paddle and the coupling body. In the first solution, numerical analysis of local stresses revealed that a redesign by changing the radius of the fillet and the radius of the groove will not reduce local stresses because of the interference of two stress raisers. In the second solution, numerical analysis of local stresses revealed that an increase in the external diameter from 340 mm to 360 mm reduced the maximum local stress by about 15% and

increased fatigue life by about 100% according to the actual estimated fatigue life. In the third solution, numerical analysis showed that a redesign of the coupling with a stiffener between the paddle and the coupling body reduced the maximum local stress and the actual service life of the couplings could be improved from the finite to the infinite lifetime.

Taking relatively a simple corrective measure of the design, such as the last one described, will greatly improve component reliability and prolong the life of components, reducing overall costs. New couplings were made by redesigning the coupling with stiffener between the paddle and the coupling body to prevent recurrence of the failure.

References

[1] Ž. Domazet, F. Lukša, M. Šušnjar. Failure analysis of rolls with grooves. Engineering Failure Analysis, Volume 14, Issues 6; September 2007, pages 1116-1174

[2] Deutsches Institut für Normung. DIN 17200. 1987 (DIN, Berlin)

[3] M. Čaušević. Obrada metala valjanjem. Veselin Masleša; Sarajevo 1983.

[4] J. Hribar. Plastična obrada metala. FSB; Zagreb 1975.

[5] Ž. Domazet, F. Lukša. Experimental determination of the rolling force on the rolls with grooves. Proceedings of the 22-nd Symposium "DANUBIA-ADRIA" on Experimental Methods in Solid Mechanics; Parma 2005.

[6] F. Lukša. Investigation of the cause of the failures of the rolls with grooves. Master Thesis, University of Split, Faculty of Electrical Engineering, Mechanical Engineering and Naval Architecture. Split 2005.

[7] Designs and technological rules "Steelworks Split". Split

[8] Metallic Materials and Elements for Aerospace Vehicle Structures. MIL-HDBK-5B, Military, Standardization Handbook. U.S. Department of Defense, 1987

[9] American Society for Testing and Materials. ASTM 322-A91. ASTM International, 2001